A 133.3 dB Dynamic Range Pulse Oximeter Front-End with Low-Noise Area-Efficient Offset Cancellation Current DAC

2023 International Conference on Electronics, Information, and Communication (ICEIC) | 979-8-3503-2021-3/23/$31.00 ©2023 IEEE | DOI: 10.1109/ICEIC57457.2023.10049972

Soungchul Park
Department of Electrical and Computer Engineering
Seoul National University
Seoul, Republic of Korea
sungchul.park@analog.snu.ac.kr

Wooyoung Kim
Department of Electrical and Computer Engineering
Seoul National University
Seoul, Republic of Korea
wooyoung.kim@analog.snu.ac.kr

Suhwan Kim
Department of Electrical and Computer Engineering
Seoul National University
Seoul, Republic of Korea
suhwan@snu.ac.kr

Jooyeol Rhee
Department of Electronic Engineering
Gachon University
Seongnam, Republic of Korea
jrhee@gachon.ac.kr

***Abstract*—This paper introduces a pulse oximeter front-end with low-noise area-efficient offset cancellation current digital-to-analog converter (DAC). The proposed offset cancellation current DAC is implemented to cancel the input DC current to improve the effective dynamic range (DR). The current DAC is designed to have low-noise and area-efficient characteristics by applying the dynamic element matching technique and reducing the number of idle current mirror transistors. It can generate a current of up to 256 µA. Due to the offset cancellation of the current DAC, the proposed pulse oximeter has a signal-to-noise ratio of 77.4 dB and an effective DR of 133.3 dB. The pulse oximeter front-end is designed in 0.13 µm CMOS and consumes 307.1 µW from a 1.65 V supply. The figure-of-merit is 0.81 pJ/Sample.**

Keywords—Analog front-end (AFE), pulse oximeter, current digital-to-analog converter (DAC), area-efficiency, wide dynamic range (DR)

I. Introduction

In recent years, various wearable devices that can monitor health status have been developed as interest in health problems increases due to the influence of pandemics [1]. Almost all the latest smart wearables and fitness trackers support pulse oximeters. A pulse oximeter is a non-invasive method to monitor blood oxygen saturation and pulse rate in real time. The pulse oximeter illuminates the skin and measures the amount of reflected light to obtain oxygen saturation [2].

The light reflected from the skin contains a DC offset signal. It is caused by various sources including ambient light and non-pulsatile structures of a body. To address the DC offset of the input signal, an offset cancellation current digital-to-analog (DAC) has been used in a pulse oximeter analog front-end (AFE) [3]–[5]. The bidirectional current DAC subtracts the DC input signal, which accounts for most of the pulse oximeter input. Canceling the DC signal enables AFE reading out of small signals of interest, thereby improving the dynamic range (DR) of the AFE. However, as the amplitude of the DC signal to be subtracted increases, the area occupied by the offset cancellation current DAC also increases. In addition, since the current DAC is placed ahead of all other conditioning circuits and directly connected to the input signal path, the considerable noise of the current DAC can significantly worsen the signal-to-noise ratio (SNR) of the pulse oximeter system.

Several works about implementing the current DAC have been proposed [6], [7]. Chopper switches have been used to apply the dynamic element matching (DEM) technique in the current generator to average mismatch errors and lower the flicker noise [6]. However, the flicker noise of the biasing transistors in the reference current branches is multiplied because only current-mirror branches are chopped. A current generator that rotates the transistors of current-mirror branches and those of reference current branches for DEM has been proposed [7]. By including the biasing transistors of the reference current branches in DEM operation, the flicker noise of the biasing transistors has also been mitigated. However, when the digital control codes are set to generate a multiplied current smaller than its maximum capability, some current branches are inevitably idle. These idle current branches can help to generate the desired output current to save chip area.

This paper presents a pulse oximeter with low-noise area-efficient offset cancellation current DAC. The proposed current DAC can significantly reduce the number of total transistors by reducing the number of idle current mirror transistors. In addition, the DEM technique attenuates the flicker noise of the current DAC, improving the noise performance of the pulse oximeter. Implemented in 0.13 µm CMOS, the proposed pulse oximeter has a DR of 133.3 dB with a DC input current compensation of up to 256 µA.

Section II explains the operating principles of the pulse oximeter. The system architecture is outlined in Section III. Next, circuit implementation is described in Section IV. Pre-layout simulation results are presented in Section V and conclusions are provided in Section VI.

II. Operating Principles

Hemoglobin (Hb) in the blood binds to oxygen and carries it to organs and tissues in the state of HbO_2. The saturation of partial pressure oxygen (SpO_2) is obtained by measuring the ratio of HbO_2 and Hb in the blood. To this end, the photoplethysmography (PPG) method is used, which transmits light of different wavelengths and detects the amount of light reflected from the body. It mainly uses red light of 660 nm wavelength and infra-red (IR) light of 940 nm

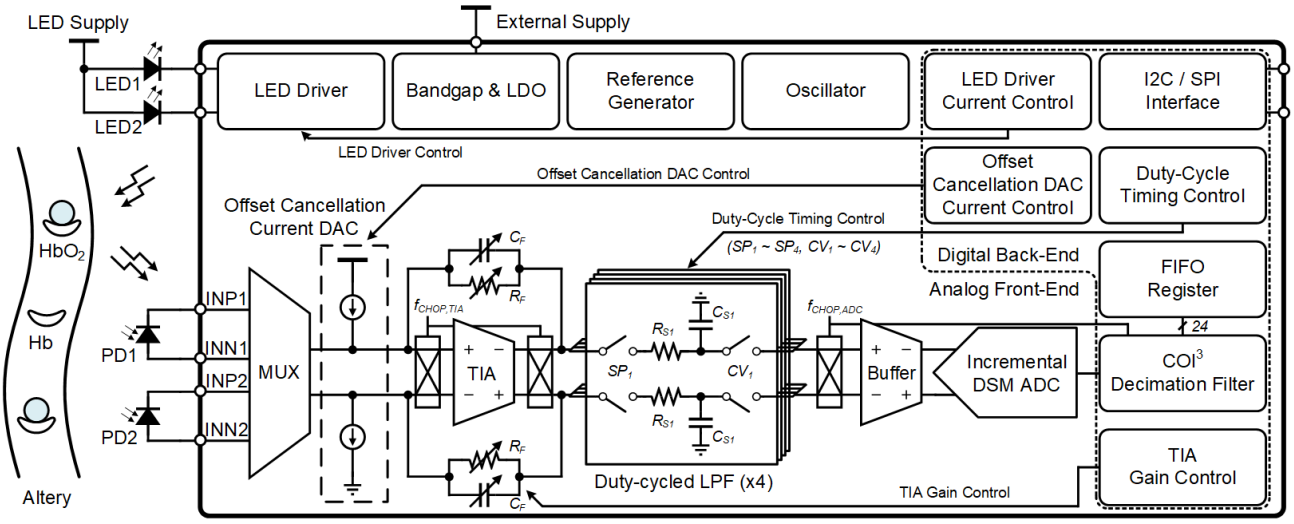

Fig. 1. Pulse oximeter front-end block diagram.

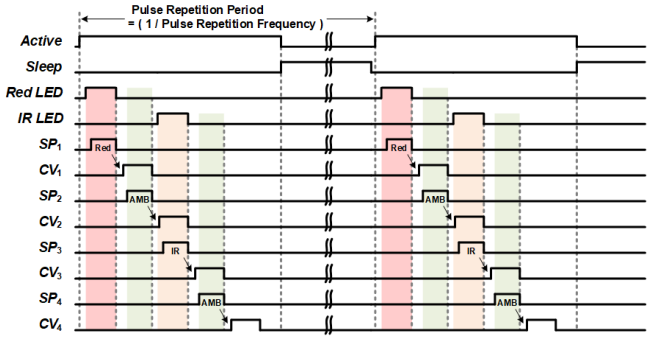

Fig. 2. Timing sequence used on pulse oximeter.

because HbO_2 and Hb have significantly different absorbance at these two lights [8]. Hb has a higher absorption rate for red light than HbO_2, while the absorption rate for IR light is lower. Some unabsorbed rays are reflected and converted to current signals via a photodiode (PD). The receiver's AFE and analog-to-digital converter (ADC) convert these currents to digital signals.

The current signal reflected from the blood vessel consists of large DC and small AC components. The AC component generated by blood circulation changes over time, while the DC components from the skin, tissue, and venous blood are relatively constant. SpO_2 can be obtained through the ratios of the AC component and the DC component, which are measured with the red light and the IR light:

$$SpO_2 = 110 - 25 \times \left(\frac{AC_{RED}}{DC_{RED}} \Big/ \frac{AC_{IR}}{DC_{IR}} \right) [\%] \qquad (1)$$

where AC_{RED}, DC_{RED}, AC_{IR}, and DC_{IR} are the AC and DC components of the red light and the IR light, respectively [9]. Typically, a value of SpO_2 is 95-100 %, and if it is less than 85 %, it may be a sign of severe hypoxemia [10].

III. System Architecture

Fig. 1 shows the structure of the pulse oximeter system. The pulse oximeter consists of a driver circuit for light-emitting diodes (LEDs), a read-out integrated circuit (ROIC) that receives the current signal from the photodiode, a digital back-end, and peripheral blocks. The LED driver can support two LEDs, and each LED current can be driven up to 200 mA through an 8-bit current control signal. Due to the differential 2-to-1 multiplexer (MUX), up to 2 photodiodes are supported. A trans-impedance amplifier (TIA) which works as an I-V converter, converts the photodiode current signal to a voltage signal. To support the programmable gain functionality, feedback resistors (R_F) are controlled from 10 kΩ to 2 MΩ by a 4-bit signal. Choppers at the input and the output of the amplifier reduce the amplifier's low-frequency noise. However, the large DC portion of the current signal limits the gain of TIA, resulting in DR degradation. The proposed low-noise area-efficient offset cancellation current DAC is implemented to subtract most of the DC signal. This allows a TIA gain of 2 MΩ improving the DR. TIA output voltage is sampled and held by duty-cycled low-pass filters (LPFs). These 4-channel anti-aliasing filters are for noise reduction and sample and hold (S&H) operation. In addition to the reflected LED light, the light entering through the photodiode has ambient light from a light source in the external environment. The duty-cycled LPF should be configured as a 4-channel to eliminate the effect of ambient light by measuring both reflected and ambient light signals.

Fig. 2 shows the timing sequence for pulse oximeter operation. First, after the LED driver turns on the red LED, the switch SP_1 is closed to sample the reflected red light signal at the sampling capacitor (C_{S1}) of the 1st LPF. Then, the red LED is turned off, SP_1 is open, and SP_2 is closed to sample the ambient light signal at C_{S2} of the 2nd LPF. In the same way, IR light and ambient light signals are sequentially sampled by the 3rd and 4th LPFs using SP_3 and SP_4 switches. Meanwhile, the sampled signal is converted to a 24-bit digital signal with the following buffer, incremental delta-sigma modulation (I-DSM) ADC, and a decimation filter. At the same time, another LPF block is being used for sampling. CV_1 is set to high, and the voltage signal sampled at C_{S1} is converted by the I-DSM ADC and stored in the FIFO register, while the 2nd LPF samples the ambient signal. In the digital back-end, the valid red light signal can be obtained by subtracting the digital code of the CV_2 phase from the digital code of CV_1. A valid IR signal can be obtained with the identical process explained above. After the above 4-channel sample and conversion process, AFE is powered down for power efficiency. The active and sleep phases are repeated every pulse repetition period (PRP).

In addition to the blocks mentioned above, the pulse oximeter has an internal oscillator, several digital controllers, I2C/SPI interfaces, and peripheral blocks, including bandgap

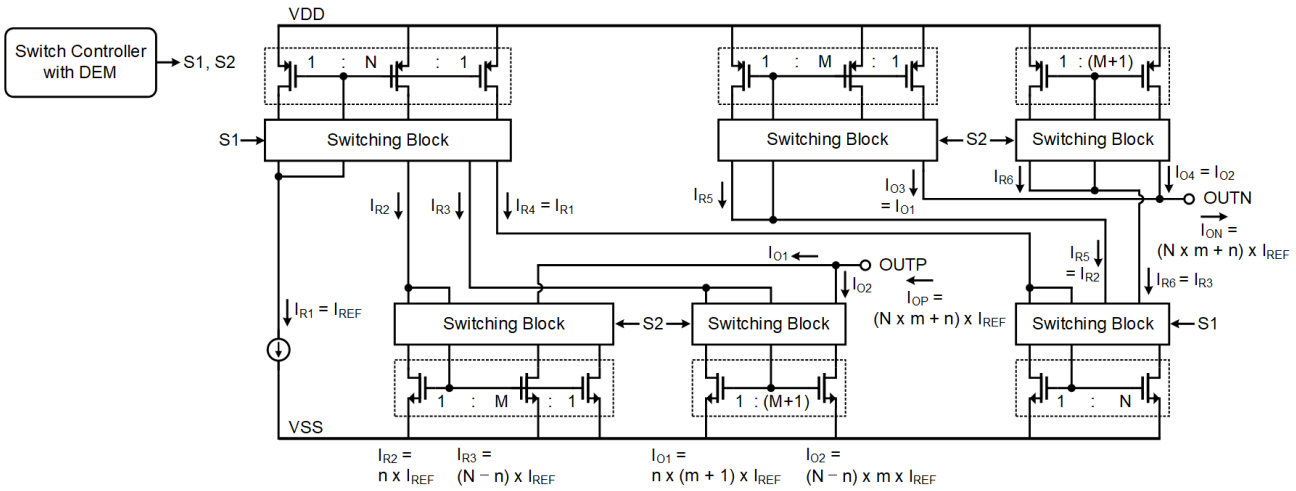

Fig. 3. Architecture of the proposed offset cancellation current DAC.

reference, low-dropout regulator (LDO), and reference generator block for stable supply voltage and bias currents.

IV. Block Implementation

A. *Offset Cancellation Current DAC*

Fig. 3 shows the structure of the proposed offset cancellation current DAC. The switch controller controls six switching blocks to generate the desired current output. The switching blocks receiving the S1 signal from the switch controller utilize all transistors in the current mirror no matter what amplitude of the desired output current is needed. Two current outputs generated by the switching block which S1 controls are calculated as follows:

$$I_{R2} = n \times I_{REF} \text{ and } I_{R3} = (N - n) \times I_{REF} \quad (2)$$

for $0 \le n \le N$ and $N \ge 2$. I_{R2} and I_{R3} are applied to different switching blocks that S2 controls, and the output currents generated from the switching blocks, I_{O1} and I_{O2}, are calculated as follows:

$$I_{O1} = n \times (m + 1) \times I_{REF} \text{ and} \quad (3)$$

$$I_{O2} = (N - n) \times m \times I_{REF} \quad (4)$$

for $0 \le m \le M$ and $M \ge 2$. The current flowing through the positive output of the current DAC, I_{OP}, is the sum of I_{O1} and I_{O2} and is expressed as follows:

$$I_{OP} = (N \times m + n) \times I_{REF}. \quad (5)$$

Similarly, the negative output of the current DAC (I_{ON}), which has the same magnitude as I_{OP} and the opposite polarity, can be obtained.

The proposed current DAC can generate output current up to N×(M+1) times I_{REF}. The total number of transistors used in the proposed current DAC is (N+2×M). In contrast, a conventional unary coded current DAC, which is designed to generate the same output current, uses N×(M+1) transistors. In the proposed DAC, N and M are chosen to be 16 and 7, respectively, so it can output up to 128 times I_{REF}. The conventional current DAC requires 128 transistors to have same output current capability, whereas the proposed current DAC requires only 30 transistors. By implementing the proposed current DAC, the total area of the current DAC including switching blocks is saved by 35.9 %.

Meanwhile, the noise of the current DAC consists of the thermal noise and the flicker noise. Since the flicker noise of the transistor is inversely proportional to the size of the transistor, DEM is applied to the switching controller. DEM technique reduces low-frequency noise as well as mismatches among unit elements. The flicker noise of the transistors is up-modulated by DEM and removed by the following duty-cycled LPF.

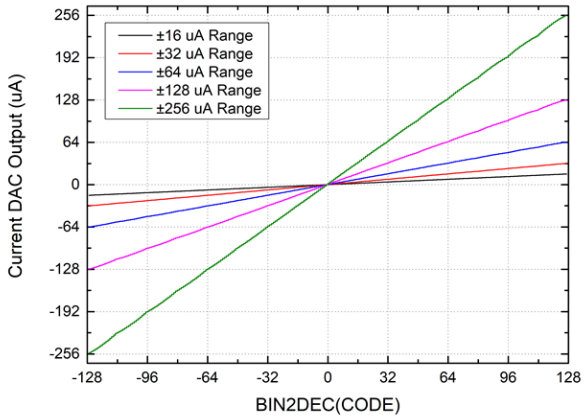

Fig. 4. Current DAC output over multiple output range settings.

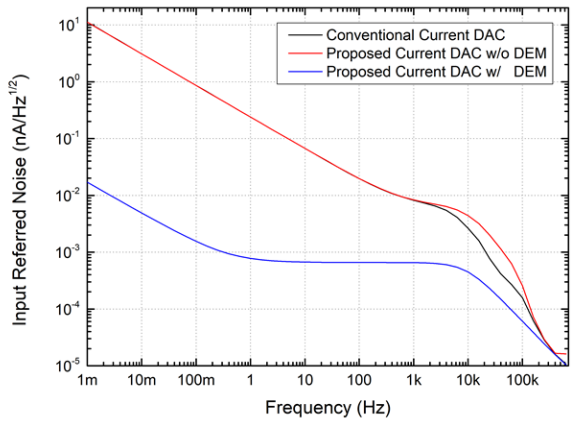

Fig. 5. Input referred-noise of the conventional current DAC and the proposed current DAC.

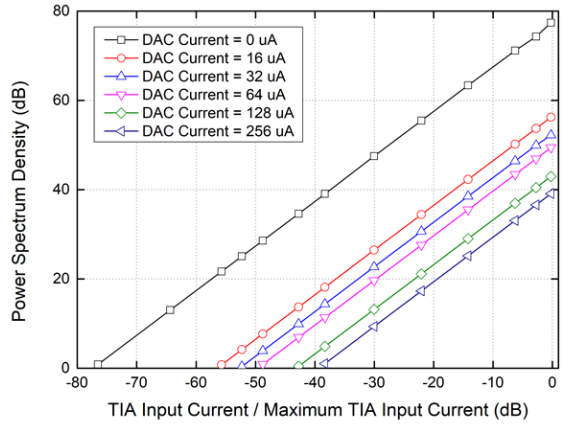

(a)

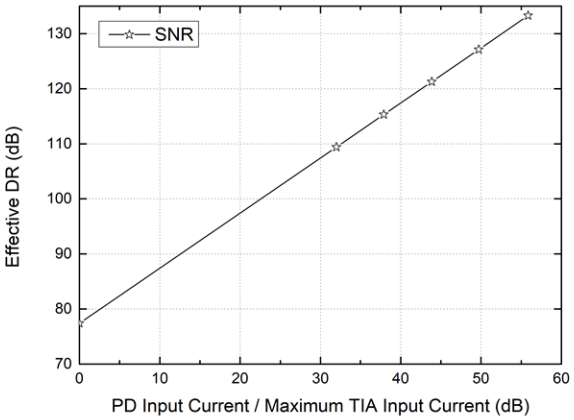

(b)

Fig. 6. (a) SNR of AFE over multiple current DAC output. (b) Effective DR of AFE over multiple current DAC output.

B. *Duty-cycled LPF*

The 4-channel duty-cycled LPF consists of resistors, sampling capacitors, and the switches SP_1 and CV_1 for sampling and conversion phases, as shown in Fig. 1. The resistors with SP_1 have been used to realize a very low bandwidth of the filter [11]. When the resistance of R_S is 1.25 MΩ, the equivalent resistance of 20 MΩ can be obtained with the duty-cycled operation. The equivalent resistance, R_{eq}, is calculated as follows:

$$R_{eq} = R_S/D = R_S/(\frac{T_{SAMP}}{PRP}) \quad (6)$$

where D is the duty of the LPF and T_{SAMP} is the time for the sampling phase. Due to the area-efficient duty-cycled LPFs, the modulated flicker noise of the current DAC can be effectively removed.

V. Simulation Results

The proposed pulse oximeter front-end was designed in 0.13 µm CMOS technology and verified in pre-layout simulations. Fig. 4 shows the output of the offset cancellation current DAC over multiple output range settings. The current output range can be switched by changing the magnitude of the reference current (I_{REF}), and the current DAC output is controlled using 8-bit signals at each output range setting. In fig. 5, the input-referred noise of the offset cancellation current DAC without and with DEM is compared with that of conventional current DAC when the output current is set to 6 µA. The flicker noise of the proposed current DAC without DEM doesn't differ much from that of the conventional current DAC. However, it can be seen that the flicker noise is decreased significantly after applying DEM to the proposed current DAC. The reason is that, as mentioned above, the low-frequency noise of the current DAC is up-modulated and then attenuated by following duty-cycled LPF. The simulated DNL and INL of the proposed current DAC are ± 0.329 LSB and ± 0.647 LSB, respectively.

TABLE I. Comparison With The Current State of the Art

	This Work	**VLSI [3]**	**SSCL [4]**	**JSSC [5]**
Technology	0.13 µm	0.18 µm	0.18 µm	0.13 µm
Supply (V)	1.65	1.2 / 3.3	1 / 2.5	1.5 / 2.5
Pulse Repetition Frequency	100 Hz	512 Hz	100 Hz	600 Hz
DC Cancellation	256 µA	200 µA	28.2 µA	10 µA
Effective DR (dB)	133.3	119	92.7	112
Gain (Ω)	10k - 2M	5k - 4M	-	19k - 90M
LED Duty cycle (%)	4.4	-	10.24	1.7
AFE Power (µW)	307.1	89	8.1	340
FOM (pJ/Sample)	0.81	0.24	2.3	1.74

Fig. 6 (a) shows the power spectrum density of the AFE when DC and AC input of 800 Hz is applied. The amplitude of the offset cancellation current DAC is set to the same value as the input DC current from the PD to compensate for the input DC current. An SNR of 77.4 dB is achieved when both input DC and DAC currents are zero. It decreases as the DAC current is set to a more considerable value due to the noise of the DAC current. The effective DR of 133.3 dB is shown in Fig. 6 (b). The effective DR of the AFE goes to its maximum point when the DAC current and the gain of the TIA are set to a maximum value.

The overall performance of the proposed pulse oximeter front-end is compared with several CMOS PPG sensor AFEs with DC cancellation current DAC [3]–[5] in Table I. The proposed AFE with low-noise area-efficient current DAC cancels an input DC current to secure a wide effective DR. It also achieves Walden's figure-of-merit (FOM) of 0.81 pJ/Sample, which shows a competitive performance.

VI. Conclusion

This paper presents a pulse oximeter front-end with low-noise area-efficient offset cancellation current digital-to-analog converter (DAC). The pulse oximeter consists of a LED driver, a read-out integrated circuit (ROIC), an internal oscillator, digital controllers, I2C/SPI interfaces, and peripheral blocks. The proposed current DAC can cancel the input DC current up to 256 µA while using only 30 transistors for current mirrors. Also, the flicker noise of the current DAC is effectively reduced by applying dynamic element matching (DEM). Due to the offset cancellation of the current DAC, the proposed pulse oximeter has a signal-to-noise ratio (SNR) of 77.4 dB and an effective dynamic range (DR) of 133.3 dB. The pulse oximeter front-end is designed in 0.13 µm CMOS and consumes 307.1 µW from a 1.65 V supply. The figure-of-merit (FOM) is 0.81 pJ/Sample.

REFERENCES

[1] X. Ding *et al.*, "Wearable sensing and telehealth technology with potential applications in the coronavirus pandemic," *IEEE Rev. Biomed. Eng.,* vol. 14, pp. 48–70, 2021.

[2] A. Jubran, "Pulse oximetry", *Crit. Care*, vol. 19, p. 272, 2015.

[3] Q. Lin *et al.*, "A 196μW, reconfigurable light-to-digital converter with 119 dB dynamic range, for wearable PPG/NIRS sensors," in *Proc. Symp. VLSI Circuits*, Kyoto, Japan, Jun. 2019, pp. C58–C59.

[4] F. Marefat, R. Erfani, and P. Mohseni, "A 1-V 8.1-μ w PPG-recording front-end with >92-dB DR using light-to-digital conversion with signal-aware DC subtraction and ambient light removal," *IEEE Solid-State Circuits Lett.*, vol. 3, no. 1, pp. 17–20, Dec. 2020.

[5] P. Schonle, F. Glaser, T. Burger, G. Rovere, L. Benini, and Q. Huang, "A multi-sensor and parallel processing SoC for miniaturized medical instrumentation," *IEEE J. Solid-State Circuits*, vol. 53, no. 7, pp. 2076–2087, Jul. 2018.

[6] H. Ko, T. Lee, J.-H. Kim, J.-A. Park, and J. P. Kim, "Ultralow-power bioimpedance IC with intermediate frequency shifting chopper," *IEEE Trans. Circuits Syst. II Express Briefs*, vol. 63, no. 3, pp. 259–263, Mar. 2016.

[7] H. Ha *et al.*, "A bio-impedance readout IC with frequency sweeping from 1 k-to-1 MHz for electrical impedance tomography," in *Proc. Symp. VLSI Circuits*, Kyoto, Japan, Jun. 2017, pp. C174–C175.

[8] Q. Lin, W. Sijbers, C. Avidikou, C. Van Hoof, F. Tavernier, and N. Van Helleputte, "Photoplethysmography (PPG) sensor circuit design techniques," in *Proc. IEEE Custom Integr. Circuits Conf.*, Apr. 2022, pp. 01–08

[9] S.-S. Oak and P. Aroul., "How to design peripheral oxygen saturation (SpO2) and. optical heart rate monitoring (OHRM) systems using the AFE4403," Texas Instruments Incorporated, Dallas, TX, USA, Tech. Rep. Appl. Rep.-SLAA655, Mar. 2015.

[10] A. T. Rheineck-Leyssius and C. J. Kalkman, "Influence of pulse oximetry settings on the frequency of alarms and detection of hypoxemia: Theoretical effects of artefact rejection, alarm delay, averaging, median filtering or lower setting of alarm limit," *J. Clin. Monit. Comput.*, vol. 14, no. 3, pp. 151–156, 1998.

[11] H. Chandrakumar and D. Markovic, "A high dynamic-range neural recording chopper amplifier for simultaneous neural recording and stimulation," *IEEE J. Solid-State Circuits*, vol. 52, no. 3, pp. 645–656, Mar. 2017.